MONITORING OF METAL FATIGUE DAMAGE USING ACOUSTIC EMISSION AND THERMOGRAPHY

DIMITRIOS G. AGGELIS, EVANGELOS Z. KORDATOS
and THEODORE E. MATIKAS
Dept. of Materials Science and Engineering, University of Ioannina, Ioannina 45110, Greece

Abstract

Acoustic emission (AE) supplies information on the fracture behavior of different materials. In this study, AE activity was recorded in metal coupons with a V-shape notch, which were loaded in fatigue until final failure. AE parameters exhibit a sharp increase approximately 1000 cycles before final failure. The use of AE parameters is discussed both in terms of characterization of the damage mechanisms and as a tool for the prediction of ultimate fatigue life. Additionally, a nondestructive methodology based on lock-in thermography is applied to determine the crack growth rate using thermographic mapping of the material undergoing fatigue. The thermographic results on the crack growth rate of aluminum alloys were then correlated with measurements obtained by the conventional compliance method, and found to be in agreement.

Keywords: Aluminum, fatigue, nondestructive evaluation, tension, shear, thermography

Introduction

Acoustic emission (AE) is a method widely used for real time monitoring of the structural condition of materials and structures [1]. The cumulative AE activity, as recorded by the sensors is indicative of the severity of cracking, since crack propagation is a prerequisite for AE in most cases. High rate of incoming signals implies the existence of several active crack sources, while low or zero activity is connected to healthy material. When several sensors are used, apart from the number of AE signals (hits), the geometric location of the cracks can be extracted due to the delay between the arrivals of the waves at different measurement points [2, 3]. This allows the estimation of which part of the structure has suffered more extensive deterioration in order to take the necessary repair action, especially for large-scale structures.

However, there are other important aspects of AE measurements, which are based on qualitative parameters of the received signals. The waveform shape depends on the cracking mode, enabling the classification of cracks in different materials [4-6]. Shear cracks generally follow tensile type as the material approaches to final failure. Therefore, crack characterization may lead to an early warning. In general, when a tensile event is occurring, the sides of the cracks move away from each other, leading to a transient volumetric change of the material and consequently most of the energy is transmitted in the form of longitudinal waves, while only a small amount in shear waves, which propagate with a lower velocity. Therefore, most of the energy is recorded quite early within the received waveform. Figure 1a shows an example of AE waveform emitted by a tensile event. The delay between the onset and the highest peak (called Rise Time, RT), is short, leading to a large rise angle of the wave. In case of a shear crack (Fig. 1b), the shape (and not the volume) of the material in the vicinity of the crack changes, shifting the proportion of energy in favor of the shear waves. Therefore, the most important part of the waveform arrives much later than the fast longitudinal arrivals, leading to longer RT and consequently a small rise angle. Recently the shape of the initial part of the waveform is examined by the RA value, which is defined as the RT over peak amplitude, A, or RA = RT/A and is measured in μs/V, as suggest-

ed by relevant recommendations [7]. Additionally, tensile events are characterized by higher frequency content, as expressed by the average frequency (AF) defined by the number of threshold crossing over the signal duration [7]. It is mentioned that these measurements depend on the "threshold", which is a value set by the user high enough in order to avoid low environmental or other noise, but at the same time sensitive enough to allow recording of the actual AE hits due to crack propagation or other material processes.
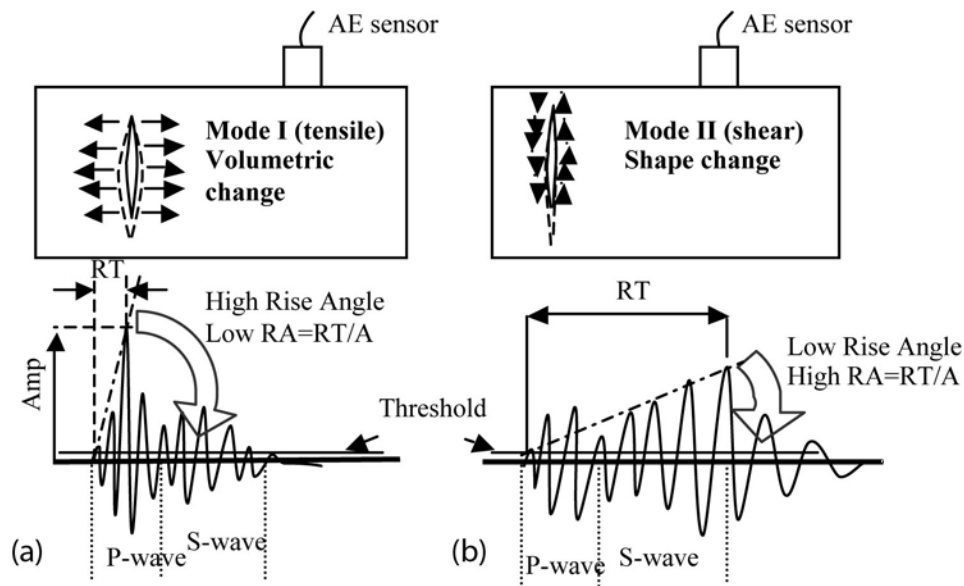
Fig. 1. Cracking modes and corresponding AE signals.

This classification scheme has proven powerful in case of laboratory applications concerning concrete cracking due to corrosion of metal reinforcing bar [5], fracture of composite laminates [4, 8], as well as the discrimination between matrix cracking and pull-out during bending of fiber reinforced concrete [9]. Specifically for the fields of metals and composites, mainly the cumulative AE activity is utilized being related to strength in single fiber-fragmentation tests [10], as well as to the remaining life in fatigue tests of steel specimens with notches [11]. Amplitude and cumulative activity have been monitored during bending of metal composite foams [12], while, concerning aluminum, AE parameters like rise time and duration have been considered in an attempt to correlate with crack growth [13, 14] and corrosive processes [15].

In this study, aluminum specimens with notches were fractured in fatigue tests. Measurements of the crack propagation rate were conducted with simultaneous AE monitoring in order to correlate the parameters obtained nondestructively with mechanical results and propose certain features as the most promising for fatigue damage characterization in metals.

Complementary to AE, infrared thermography was applied to monitor the cracking procedure during the fatigue of the same specimens. Infrared thermography is a powerful nondestructive evaluation tool, which can be effectively used for defect detection in materials such as aluminum alloys. In the industry, where inspection is of paramount importance in all fabrication stages, there is a need for fast, reliable nondestructive assessment techniques. Infrared lock-in thermography can fulfill this need because it is a quick, full-field and real-time inspection tool, which can examine a relatively large area of a structure. It is also a noncontact technique; the equipment is fairly portable and hence can be used reasonably easily in the field [16]. Lock-in thermography provides a powerful tool to study thermo-mechanical mechanisms. Instead of a simple tempera-

ture rise measurement, which depends on environmental conditions, lock-in thermography locates and measures thermal sources, which are proportional to thermo-mechanical energy, under harmonic loading and adiabatic conditions [17]. A major advantage of IR thermography applications is the detection and monitoring of sub-surface cracking [18-20].

In this paper, the fatigue crack propagation was monitored using a method, which was developed in previous work [21, 22] based on infrared lock-in thermography. The crack-tip stress field has been mapped using thermoelasticity principles. This technique is based on the fact that stresses within a solid material result in variations of the temperature. When the material is under tensile load, its temperature decreases proportionally to the load. However, when it is under compressive load, its temperature increases proportionally to the load. This behavior is known as the thermoelastic effect [17]. The setup included a radiometric camera, which measured the infrared radiation produced on the surface of the material undergoing cyclic loading, and a real-time correlator called "lock-in module", which measured the change of temperature extracting it from the noise that is specified by the thermal resolution of the camera. Lock–in refers to the necessity to monitor the exact time-dependence between the output signal and the reference input signal [23]. This was done using a lock–in amplifier so that both phase and magnitude images become available. When the material becomes deformed, a part of the energy necessary to propagate the damage is transformed into heat [24, 25]. The heat wave, generated by the thermo-mechanical coupling and the intrinsic dissipated energy during mechanical loading of the sample, was detected by the thermographic camera.

Experimental Procedure

Materials and mechanical testing
The material was aluminum (AA7075). This material exhibits good resistance to corrosion, and high strength in environment as well as at high temperatures. Test specimens were manufactured according to ASTM E399-09e1. For the determination of the crack propagation rate (CPR) a crack opening displacement (COD) gage is fixed in the notch opening. The determination of crack propagation rate followed ASTM E647-08e1. The fatigue tests were conducted on an Instron servo-hydraulic machine with maximum static and dynamic load of ±100 kN. The fatigue cycle was sinusoidal with frequency of 3 Hz, the stress ratio ($Load_{max}/Load_{min}$) was set to R = 0.2 and the amplitude ($Load_{max} - Load_{min}$) = 4 kN.

Acoustic emission
Two piezoelectric sensors (Pico, Physical Acoustics Corp., PAC) were attached on one side of the specimen (see Fig. 2). The sensors were attached using wax, which enhanced acoustic coupling, while supporting the sensors throughout the experiment. The frequency bandwidth is within 50 to 800 kHz and therefore, the sensors are suitable for monitoring of different sources. The AE signals were recorded on two channels in a PAC-PCI-2 board with a sampling rate of 5 MHz. The software used was PAC AEWin, with AE activity and the signal parameters monitored in real time. The whole waveform data were recorded for post-processing.

Thermography
Lock-in IR thermography was used for non-contact monitoring of the crack propagation during the test. Thermographic assessment of fracture enabled determination of the crack growth rate. An infrared camera was placed at a distance from the specimen. The IR camera was connected with the lock-in amplifier and the amplifier with the main servo-hydraulic controller (see Fig. 3). Therefore, synchronization of the frequency through the lock-in amplifier and the testing

machine could be achieved and lock-in images and data capture during the fatigue testing were enabled. The experiments were conducted using an infrared camera CEDIP (MIW) with a cooled indium antimonide (InSb) detector (3-5 μm), a frame rate of 150 Hz and a focal plane array (FPA) with pixel format of 320 (H) x 240 (V). The resolution of the IR camera was 20 mK and the integration time is 1.5 ms.
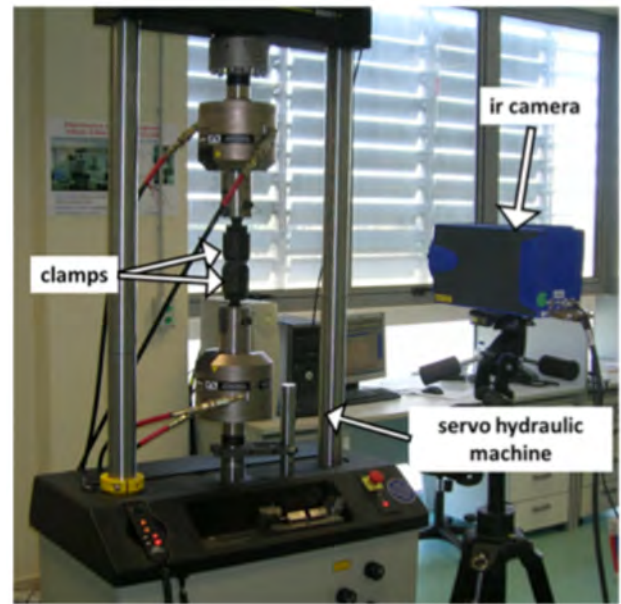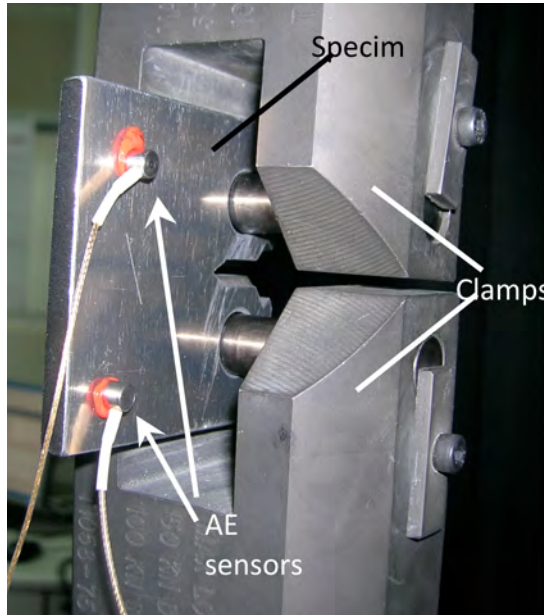
Fig. 2. Photograph of the sensors on the specimen. Fig. 3. Photograph of the experimental setup.

Results

Acoustic emission
Figure 4 shows the crack propagation rate (da/dN) as a function of time. As typically expected in metal fatigue the rate increases exponentially. The final failure of the specimen occurred at 3231 s. AE monitoring presented a more or less constant activity throughout the experiment. AE signals are recorded shortly after the start of the test. Without many fluctuations, the AE hit rate can be characterized as constant leading to a total number of almost 20000 hits.
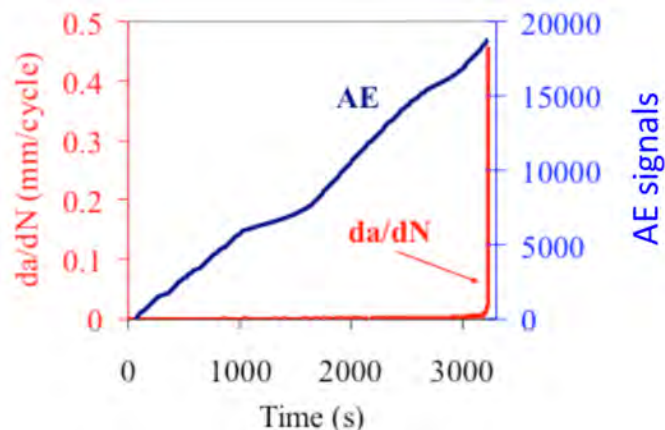
Fig. 4. Time history of CPR (or da/dN) and cumulative AE.

However, other AE parameters show a very distinct and clear trend. Figure 5 presents the duration and rise time of the signals. It is clear that approximately 200 to 300 s before the final

fracture, the duration and RT start to increase sharply. Specifically, until 3000 s the duration of the acquired signals was typically less than 3000 μs, while the RT less than 500 μs. After that point, AE signals with much longer duration and RT are recorded, as seen by the cloud of points rising to the top of the figure before the final fracture.
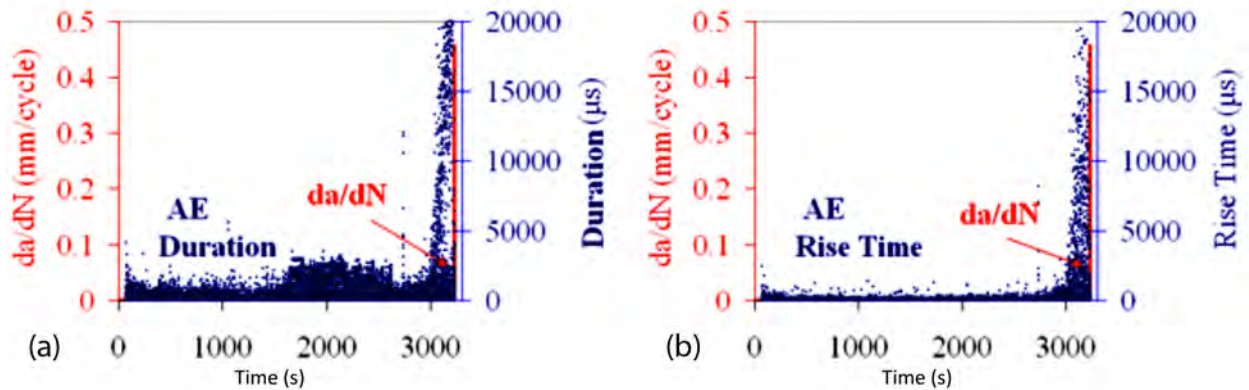
Fig. 5. Time history of CPR and (a) AE duration (b) RT.

The increasing duration and RT indicate possible shift of the cracking mode from tensile to shear. As mentioned above, this transition between different cracking modes can be examined by the RA value [7], which also takes into account the signals' amplitude. RA history in relation to the CPR can be seen in Fig. 6 for the last stage of the specimen's life (after 2500 s).
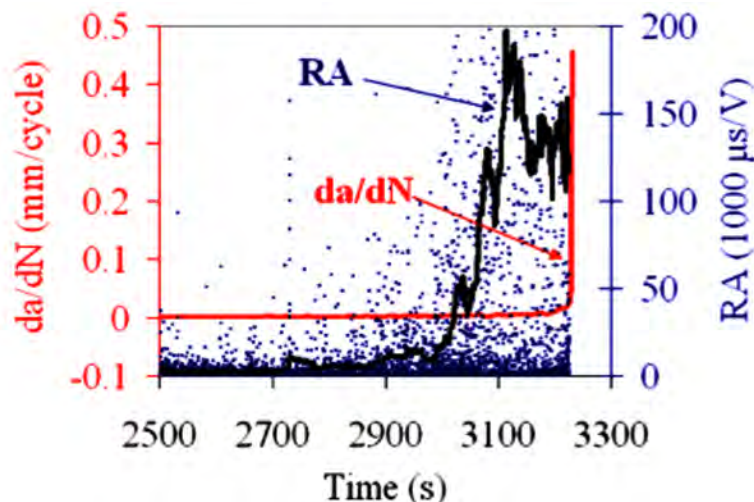
Fig. 6. Time history of CPR and RA.

Before 2700 s, RA values higher than 50 ms/V are infrequent. However, after 2900 s, the population of points expand to values higher than 75 ms/V. The solid line stands for the moving average of the recent 150 hits, which shows a clear increase at 3000 s, much earlier than the specimen's fracture. As discussed above, this shift of the RA value implies also the shift between the tensile and shear fracture modes; actually this is the sequence of the cracking modes within a typical fatigue specimen of this kind. Figure 7a shows a photograph of the fracture surface after the end of the experiment. The crack propagates horizontally for approximately 20 mm from the notch. Later, the fracture surface becomes curved. This is attributed of the local plane stress field. Due to the small thickness of the plate, the stress perpendicular to the surface (σ_Z) is zero (Fig. 7b). Therefore, although the crack starts to propagate horizontally dictated by the notch, under the application of the tensile stress (σ_Y), final fracture occurs due to the shear stresses,

which are maximum at 45°. This cracking mode sequence is responsible for the behavior of the AE parameters. The small specimen size and the sensitivity of the sensors enable the capture of these changes accurately as the crack propagates.
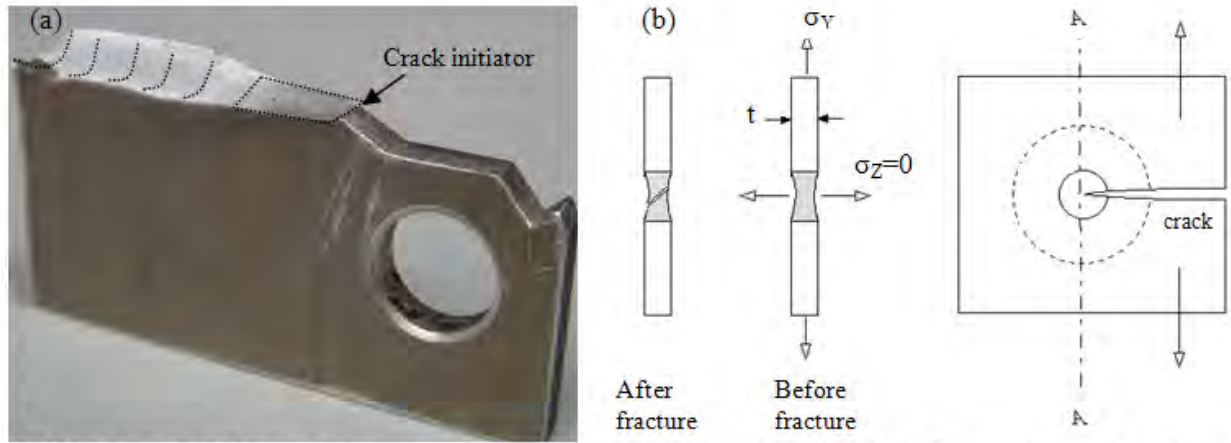
Fig. 7. (a) Part of the specimen after fatigue failure. (b) Plane stress fracture.

Another AE parameter that has been employed in cracking mode classification is the average frequency, AF, as mentioned earlier. In the present study, this parameter exhibits shifting trends, but in a much smoother way than RA. Figure 8 shows the AF of all hits as well as the linear fit to the data. The linear fit is produced to show the smooth but clear decreasing trend, which cannot be visually evaluated by the dispersed cloud of points. Indeed, there is a shift from an average value of 83 kHz at the beginning of the loading to approximately 50 kHz at fracture. This decrease can be again connected to the change of the dominant crack mode from tension to shear. The observed AE behavior is repeatable for all five specimens tested with parameters, such as RT, RA and AF.
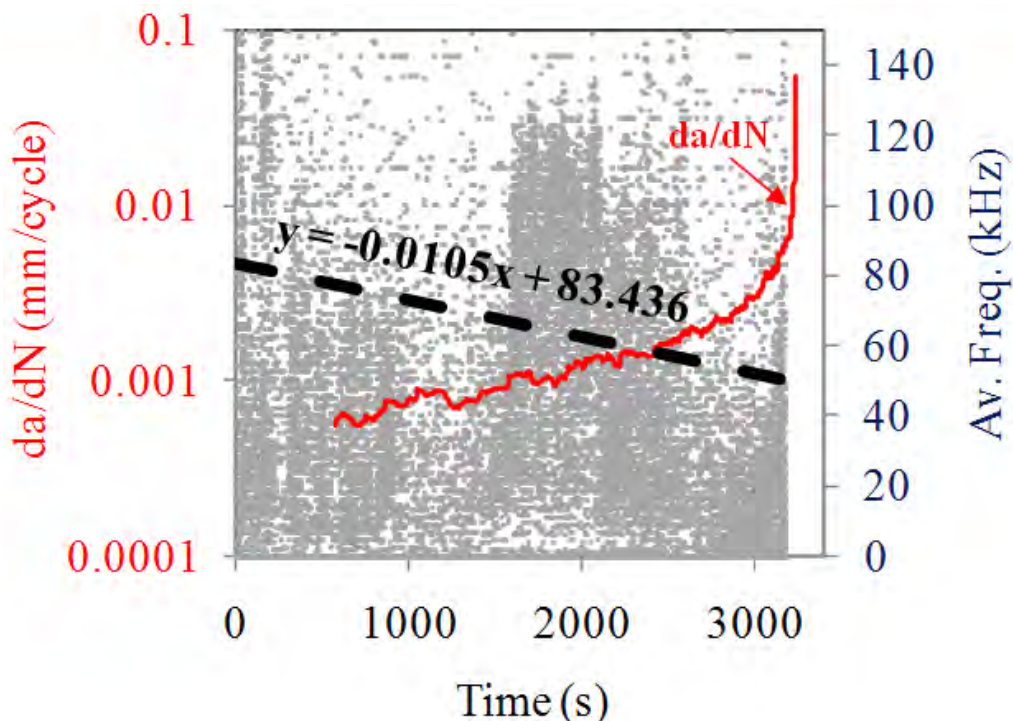
Fig. 8. Time history of CPR and AF.

Lock-in thermography results

In order to determine the crack growth rate using thermographic mapping of the material undergoing fatigue, we applied a specific procedure, which was described extensively in previous work [20]. According to this procedure, the distribution of temperature and stresses at the surface of the specimen was initially monitored during the test. The thermal images were obtained as a function of time (cycles). The stresses were determined in a post-processing mode based on thermoelasticity theory, as stated in the introduction, and the thermal variations monitored on the surface of the coupon. Local stresses versus time were measured along each of the fifteen reference lines (see Fig. 9a) drawn on the thermograph in front of the notch. The method was applied in five AA7075 specimens.

The maximum values of stress for three different reference lines of the fifteen are depicted against the number of fatigue cycles in Fig. 9b. The local stress is monitored at the location of each line. First, it increased while the crack approached the line, and attained a maximum value when the crack tip crossed the line. After the crack crossed the line, the local stress decreased.

The exact time and the corresponding fatigue cycle that each line attains a maximum value of stress can be defined by the plot of Fig. 9b (see arrows). All the reference lines had been drawn on the thermograph at fixed position in front of the crack-starting notch. Therefore, the crack growth rate (da/dN) can be calculated from the exact positions (mm) of reference lines and the fatigue cycle when the crack reaches each reference line.
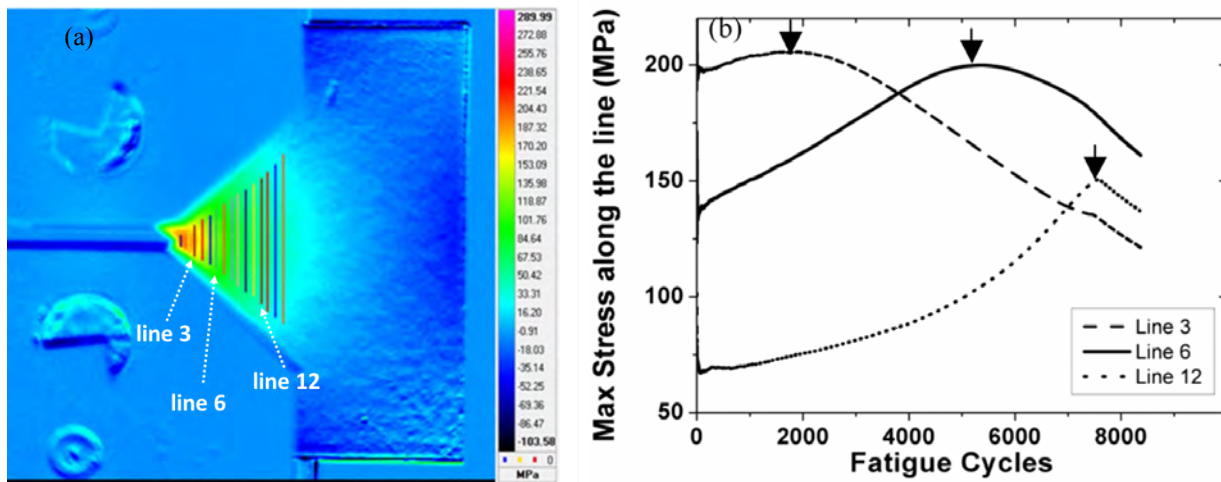
Fig. 9. (a) thermograph of 3 plotted reference lines s, (b) Diagram of max stress along 3 typical reference lines vs. fatigue cycle.

The crack growth rate values of aluminum alloy AA7075 obtained by the conventional compliance method were correlated with the damage parameters obtained using lock-in thermography (see Fig. 10). As can be seen by the thermographic data there is an abrupt change of the damage parameter after approximately 8000 cycles, indicating the upcoming failure of the specimen at approximately 80% of its total fatigue life. Observing this figure, it can be concluded that the lock-in thermography index can be regarded as a prediction of the crack propagation rate measured by the compliance method in AA7075 aluminum alloys. Specifically IR thermography indicates incipient catastrophic failure at approximately 80% of the fatigue life.
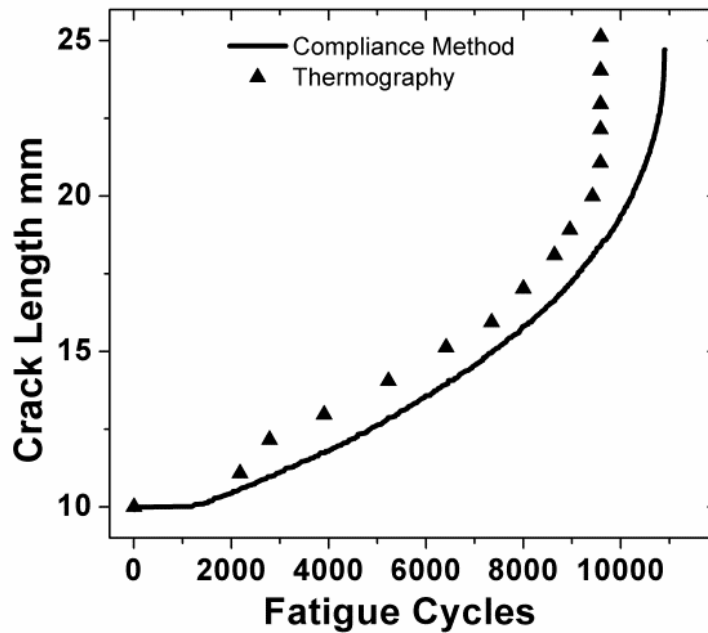
Fig. 10. Crack length vs. fatigue cycles determined by the compliance method and thermography.

Conclusion

This paper presents preliminary results on the AE monitoring during fatigue of aluminum coupons. The aim is the correlation of AE parameters with damage accumulation and the fracture mode. Study of the AE behavior shows that certain characteristics undergo clearly measureable changes much earlier than final fracture. Specifically, among others, the duration and the rise time of the signals, as well as the RA value of the waveforms increase sharply approximately 1000 to 1200 cycles before final failure. The mechanism, which is responsible for this change, seems to be the shift from the tensile to shear fracture mode. Such shift typically occurs in thin metal coupons with a notch. This is well known by visual observation of the specimen's fracture surface. It is concluded that these AE parameters should be further studied in order to establish early warning sign against final fracture and to characterize the damage status at any point of the materials life.

Additionally, this work demonstrated that crack growth rate can be effectively monitored by using lock-in thermography in metallic materials undergoing cyclic loading. The results obtained using this nondestructive technique were in agreement with the conventional compliance method. Thermographic monitoring is a noncontact, full-field, method able to assess accurately crack growth even in cases that cracking is not visible on the specimen's surface and propagates inside the material. In addition, it can be concluded that the new method, based on IR thermography, enables prediction of upcoming catastrophic failure of the specimen at an early state of damage. Lock-in IR thermography has a significant advantage since it can be used in situations which the conventional compliance method cannot be applied.

References

[1] Grosse, C. U. and Ohtsu, M., 2008. *Acoustic Emission Testing*, Springer, Heidelberg.

[2] Aggelis D.G., Shiotani T., Momoki S. and Hirama A., 2009. "Acoustic Emission and Ultrasound for Damage Characterization of Concrete Elements". ACI Materials J. **106**(6), 509-514.

[3] Grosse, C., Reinhardt, H. and Dahm, T., 1997. "Localization and classification of fracture types in concrete with quantitative acoustic emission measurement techniques", NDT&E Int. **30**(4), 223-230

[4] Anastassopoulos, A.A. and Philippidis, T.P., 1994. "Clustering Methodology for Evaluation of Acoustic Emission from Composites". J. Acoustic Emission **13**(1/2), 11-22.

[5] Ohtsu, M. and Tomoda, Y., 2007. "Phenomenological model of corrosion process in reinforced concrete identified by acoustic emission". ACI Mater J. **105**(2), 194–200.

[6] Shiotani, T., Ohtsu, M. and Ikeda, K., 2001. "Detection and evaluation of AE waves due to rock deformation". Construction and Building Materials, **15**(5-6), 235-246.

[7] Ohtsu M., 2010. Recommendation of RILEM TC 212-ACD: Acoustic emission and related NDE techniques for crack detection and damage evaluation in concrete: Test method for classification of active cracks in concrete structures by acoustic emission, Materials and Structures, **43**(9), 1187-1189.

[8] Aggelis, D.G., Barkoula, N.M., Matikas, T.E. and Paipetis, A.S., 2010. "Acoustic emission monitoring of degradation of cross ply laminates". J. Acoust. Soc. Am. **127**(6), EL246-251.

[9] Soulioti, D.V., Barkoula, N.M., Paipetis, A.S., Matikas, T.E., Shiotani, T. and Aggelis, D.G., 2009. "Acoustic emission behaviour of steel fibre reinforced concrete under bending". Construction and Building Materials **23**, 3532-3536.

[10] Rousset, G., Martin, E. and Lamon J., 2009. "In situ fibre strength determination in metal matrix composites", Composite Science and Technology **69**, 2580-2586.

[11] Roberts, T.M. and Talebzadeh, M., 2003a. "Acoustic emission monitoring of fatigue crack propagation". Journal of Constructional Steel Research **59**, 695-712.

[12] Brown, J., A., Vendra, L. J. and Rabiei, A., 2010. Bending Properties of Al-Steel and Steel-Steel Composite Metal Foams. Metallurgical and Materials Transactions A, **41A**, 2784-2793.

[13] Aggelis, D. G., Kordatos, E. Z., Matikas, T. E. 2010. Monitoring of acoustic emission during fatigue of metal plates, *Progress in Acoustic Emission XV*, ed. Wakayama et al. JSNDI 2010, pp. 73-78.

[14] Aggelis, D. G., Kordatos, E. Z., Matikas. T. E. 2011. Acoustic emission for fatigue damage characterization in metal plates, Mechanics Research Communications, **38**, 106-110.

[15] Boinet, M., Bernard, J., Chatenet, M., Dalard, F. and Maximovitch, S., 2010. "Understanding aluminium behaviour in aqueous alkaline solution using coupled techniques Part II: Acoustic emission study", Electrochimica Acta **55**, 3454-3463.

[16] Wong, B.S., Tui, C.G., Bai, W., Tan, P.H., Low, B.S., Tan, K.S. 1999. Thermographic evaluation of defects in composite materials. Insight: Non-Destructive Testing and Condition Monitoring, **41**(8), 504-9.

[17] Brémond, P., Potet, P. 2001. Lock-in thermography: A tool to analyse and locate thermo-mechanical mechanisms in materials and structures. In: *Proc. SPIE 4360*, *Thermosense XXIII*. Rozlosnik, A.E., Dinwiddie, R.B., editors. SPIE Press, Orlando, FL, 2001, 560-566.

[18] Yang, B., Liaw, P.K., Wang, G., Peter, W.H., Buchanan, R.A., Yokoyama, Y. 2004. Thermal-Imaging Technologies for Detecting Damage during High-Cycle Fatigue. Metallurgical and Materials Transactions A: Physical Metallurgy and Materials Science, **35**A(1), 15-23.

[19] Plekhov, O., Palin-Luc, T., Saintier, N., Uvarov, S., Naimark, O. 2005. Fatigue crack initiation and growth in a 35CrMo4 steel investigated by infrared thermography. Fatigue and Fracture of Engineering Materials and Structures, **28**(1-2), 169-178.

[20] Ait Aouit, D., Ouahabi, A. 2008. Monitoring crack growth using thermography. Suivi de fissuration de matériaux par thermographie, **336**(8), 677-683.

[21] Kordatos, E.Z., Myriounis, D.P., Hasan, S.T., Matikas, T.E. 2009. Monitoring the fracture behavior of SiCp/Al alloy composites using infrared lock-in thermography. Proc. SPIE 7294, 72940X.

[22] Myriounis, D.P., Kordatos, E.Z., Hasan, S.T., Matikas, T.E. 2011. Crack-Tip Stress Field and Fatigue Crack Growth Monitoring Using Infrared Lock-In Thermography in A359/SiCp Composites. Strain, **47**, e619-e27.

[23] Maldague, X.V. 2001. Theory and practice of infrared technology for nondestructive testing, John Wiley & Sons Inc, New York.

[24] Choi, M-Y., Park, J-H., Kang, K-S., Kim, W-T. 2006. Application of thermography to analysis of thermal stress in the NDT for compact tensile specimen. Proc 12th PCNDT 2006.

[25] ASM Handbook. 1989. Nondestructive Evaluation and Quality Control, Vol.17.